

# Stability of Trivalent Vanadium Alkyl and Hydride Supported by a Chelating Phosphinimido Ligand

Ghazar Aharonian, Khalil Feghali, Sandro Gambarotta,\* and Glenn P. A. Yap

Department of Chemistry, University of Ottawa, Ottawa, Ontario, Canada

Received February 27, 2001

Reaction of  $[(\text{Me}_3\text{Si})\text{N}=\text{P}(\text{Ph})_2\text{C}(\text{H})\text{P}(\text{Ph})_2=\text{N}(\text{SiMe}_3)]\text{VCl}_2$  (**1**) with 2 equiv of MeLi yielded the corresponding trivalent vanadium derivative  $[(\text{Me}_3\text{Si})\text{N}=\text{P}(\text{Ph})_2\text{C}(\text{H})\text{P}(\text{Ph})_2=\text{N}(\text{SiMe}_3)]\text{VMe}_2$  (**3**). Subsequent hydrogenolysis afforded the dinuclear hydride complex  $\{[(\text{Me}_3\text{Si})\text{N}=\text{P}(\text{Ph})_2\text{C}(\text{H})\text{P}(\text{Ph})_2=\text{N}(\text{SiMe}_3)]\text{V}\}_2(\mu\text{-H})_2$  (**4**), where reduction of the metal center to the divalent state had occurred. Hydrogenolysis of solutions of **1** previously treated with lower than stoichiometric amounts of MeLi afforded the two mixed-valent V(II)/V(III) hydrides  $\{[(\text{Me}_3\text{Si})\text{N}=\text{P}(\text{Ph})_2\text{C}(\text{H})\text{P}(\text{Ph})_2=\text{N}(\text{SiMe}_3)]\text{V}\}_2(\mu\text{-Cl})_2(\mu\text{-H})$  (**6**) and  $\{[(\text{Me}_3\text{Si})\text{N}=\text{P}(\text{Ph})_2\text{C}(\text{H})\text{P}(\text{Ph})_2=\text{N}(\text{SiMe}_3)]\text{V}\}_2(\mu\text{-Cl})(\mu\text{-H})_2$  (**7**). Hydrolysis of the divalent **4** afforded the trivalent and dinuclear  $\{[(\text{Me}_3\text{Si})\text{N}=\text{P}(\text{Ph})_2\text{C}(\text{H})\text{P}(\text{Ph})_2=(\mu\text{-N})\text{V}(\text{OSiMe}_3)]\}_2$  (**5**), featuring migration of the  $\text{Me}_3\text{Si}$  group from the N to the O atom of one incoming molecule of water.

## Introduction

Binary vanadium hydrides in medium-valent oxidation states are important compounds, displaying a wide range of useful applications in solid-state chemistry,<sup>1</sup> electrochemistry,<sup>2</sup> hydrogen storage devices,<sup>3</sup> etc. Thus, a wealth of reactivity can reasonably be expected for molecular vanadium hydrides also in view of the remarkable behavior displayed by the heavier Nb and Ta congeners.<sup>4</sup> Nevertheless, medium-valent vanadium hydrides remain rare,<sup>5</sup> despite the promising behavior displayed by some of the few existing examples.<sup>5,6</sup>

There is another point of interest that makes the availability of di- and trivalent vanadium hydrides particularly desirable. Trivalent vanadium complexes are used as catalysts for the commercial production of elastomers.<sup>7</sup> One of the problems encountered during the polymerization reaction is the reduction of the metal center to the inactive divalent state.<sup>8</sup> This reaction,

which is responsible for catalyst failure and deactivation, is believed to occur via  $\beta$ -hydrogen elimination of the growing chain and consequent formation of unstable vanadium hydrides. Therefore, identifying the factors which affect the stability of mid-valent vanadium hydrides may have some important implications for catalyst design and improvement.

A few years ago we reported the hydrogenolysis of a cyclometalated trivalent vanadium silazanate species in the presence of phosphine.<sup>9</sup> The reaction afforded a cationic divalent vanadium polyhydride. This result indicates that trivalent vanadium hydride, supported by monodentate amide and generated in the early stage of the hydrogenolysis, may possess some intrinsic instability. On the other hand, the successful characterization by Cloke of a stable trivalent hydrido-bridged vanadium complex<sup>10</sup> stabilized by tridentate amide ligand, also silylated, strongly suggests that ligand

(1) See for example: (a) Dus, R.; Nowicka, E.; Wolfram, Z. *Langmuir* **1998**, *14*, 5487. (b) Paniago, R.; Schmid, S.; Metzger, T. H.; Chow, P. C.; Reichert, H.; Moss, S. C.; Peisl, J.; Liang, K. S. *Physica B* **1996**, *221*, 210. (c) Maitre, P.; Bauschlicher, C. W., Jr. *J. Phys. Chem.* **1995**, *99*, 6836.

(2) See for example: (a) Tsukahara, M.; Takahashi, K.; Mishima, T.; Miyamura, H.; Sakai, T.; Kuriyama, N.; Uehara, I. *J. Alloys Compd.* **1995**, *231*, 616. (b) Tsukahara, M.; Takahashi, K.; Mishima, T.; Sakai, T.; Miyamura, H.; Kuriyama, N.; Uehara, I. *J. Alloys Compd.* **1995**, *231*, 226. (c) Yang, H. W.; Wang, Y. Y.; Wan, C. C. *J. Electrochem. Soc.* **1996**, *143*, 429. (d) Zuetzel, A.; Meli, F.; Chartouni, D.; Schlapbach, L.; Lichtenberg, F.; Friedrich, B. *J. Alloys Compd.* **1996**, *239*, 175.

(3) See for example: (a) Gao, X. P.; Zhang, W.; Yang, H. B.; Song, D. Y.; Zhang, Y. S.; Zhou, Z. X.; Shen, P. W. *J. Alloys Compd.* **1996**, *235*, 225. (b) Iwakura, C.; Choi, W. K.; Miyauchi, R.; Inoue, H. *J. Electrochem. Soc.* **2000**, *147*, 2503. (c) Tsukahara, M.; Kamiya, T.; Takahashi, K.; Kawabata, A.; Sakurai, S.; Shi, J.; Takeshita, H. T.; Kuriyama, N.; Sakai, T. *J. Electrochem. Soc.* **2000**, *147*, 2941.

(4) See for example: (a) Fryzuk, M. D.; Johnson, S. A.; Rettig, S. *Organometallics* **2000**, *19*, 3931. (b) Mulford, D. R.; Clark, J. R.; Schweiger, S. W.; Fanwick, P. E.; Rothwell, I. P. *Organometallics* **1999**, *18*, 4448. (c) Fryzuk, M. D.; Johnson, S. A.; Rettig, S. *J. Am. Chem. Soc.* **1998**, *120*, 11024. (d) Parkin, B. C.; Clark, J. R.; Viscigillo, V. M.; Fanwick, P. E.; Rothwell, I. P. *Organometallics* **1995**, *14*, 3002. (e) Tayebani, M.; Gambarotta, S.; Yap, G. *Organometallics* **1998**, *17*, 3639. (f) Tayebani, M.; Feghali, K.; Gambarotta, S.; Yap, G. *Organometallics* **1998**, *17*, 4282. (g) Berno, P.; Gambarotta, S. *Organometallics* **1995**, *14*, 2159.

(5) (a) Jonas, K.; Wiskamp, V.; Tsay, Y. H.; Kruger, C. *J. Am. Chem. Soc.* **1983**, *105*, 5480. (b) Bansemir, R. L.; Huffman, J. C.; Caulton, K. G. *J. Am. Chem. Soc.* **1983**, *105*, 6163. (c) Greiser, T.; Puttfarcken, U.; Rehder, D.; *Transition Met. Chem.* **1979**, *4*, 168. (d) Herrmann, W. A.; Biersack, H.; Balbach, B.; Wulknitz, P.; Ziegler, M. L. *Chem. Ber.* **1984**, *117*, 79. (e) Hessen, B.; Van Bolhuis, F.; Teuben, J. H.; Peterson, J. L. *J. Am. Chem. Soc.* **1988**, *110*, 295. (f) Hessen, B.; Meetsma, A.; Teuben, J. H. *J. Am. Chem. Soc.* **1989**, *111*, 5977. (g) Hessen, B.; Buijink, J. K. F.; Meetsma, A.; Teuben, J. H.; Helgesson, G.; Hakansson, M.; Jagner, S. *Organometallics* **1993**, *12*, 2268. (h) Gardner, T. G.; Girolami, G. S. *Organometallics* **1987**, *6*, 2551. (i) Arrieta, J. M. *Polyhedron* **1992**, *11*, 3045.

(6) Sussmilch, F.; Olbrich, F.; Rehder, D. *J. Organomet. Chem.* **1994**, *481*, 125.

(7) See for example: (a) Desmangles, N.; Gambarotta, S.; Bensimon, C.; Davis, S.; Zahalka, H. *J. Organomet. Chem.* **1997**, *562*, 53. (b) Kim, W. K.; Fevola, M. J.; Liable-Sands, L. M.; Rheingold, A. L.; Theopold, K. H. I. *Organometallics* **1998**, *17*, 4541. (c) Davis, S. C.; Van Hellens, W.; Zahalka, H. In *Polymer Material Encyclopedia*; Salamone, J. C., Ed.; CRC Press: Boca Raton, FL, 1996; Vol. 3. (d) Addison, E. *J. Polym. Sci., A: Polym. Chem.* **1994**, *32*, 1033. (e) Gumboldt, A.; Helberg, J.; Schleitzer, G. *Makromol. Chem.* **1967**, *101*, 229. (f) Ouzumi, T.; Soga, K. *Makromol. Chem.* **1992**, *193*, 823. (g) Doi, Y.; Suzuki, S.; Soga, K. *Macromolecules* **1986**, *19*, 2896.

(8) See for example: Reardon, D.; Conan, F.; Gambarotta, S.; Yap, G.; Wang, Q. *J. Am. Chem. Soc.* **1999**, *121*, 9318 and references cited therein.

(9) Berno, P.; Gambarotta, S. *Angew. Chem., Int. Ed. Engl.* **1995**, *34*, 822.

denticity rather than electronic factors affects the stability of trivalent vanadium hydrides.

Herein, we describe the preparation and characterization of three rare examples of divalent and mixed-valence vanadium hydrides as well as of a trivalent alkyl. The ligand system selected for this work was the pincer-type bis-phosphinimide anion  $(\text{Me}_3\text{Si})\text{N}=\text{P}(\text{Ph})_2\text{-CHP}(\text{Ph})_2=\text{N}(\text{SiMe}_3)^{11}$  because of its tridentate and tripodal-like bonding mode and the electronic flexibility provided by the delocalization of the negative charge between the deprotonated carbon and the two nitrogen atoms. Also desirable was the presence of the  $\text{P}=\text{N}$  function, which is well known to support both a very high level of catalytic activity<sup>12</sup> and to stabilize a large variety of metal complexes and oxidation states.<sup>13</sup>

## Experimental Section

All operations were performed under an inert atmosphere by using standard Schlenk-type techniques.  $\text{VCl}_3(\text{THF})_3$ <sup>14</sup> and  $\text{H}_2\text{C}(\text{PPh}_2\text{NSiMe}_3)_2$ <sup>15</sup> were prepared according to published procedures. Methylolithium (1.4 M solution in ether) was obtained from Aldrich and was used as received. Infrared spectra were recorded on Mattson 9000 and Nicolet 750-Magna FTIR instruments from Nujol mulls prepared in a drybox. Samples for magnetic susceptibility measurements were weighed inside a drybox equipped with an analytical balance and sealed into calibrated tubes. Magnetic measurements were carried out with a Gouy balance (Johnson Matthey) at room temperature. Magnetic moments were calculated following standard methods,<sup>16</sup> and corrections for underlying diamagnetism were applied to the data.<sup>17</sup> Elemental analyses were carried out with a Perkin-Elmer 2400 CHN analyzer. Data for X-ray crystal structure determination were obtained with a Bruker diffractometer equipped with a Smart CCD area detector.

**Preparation of  $[\text{CH}(\text{PPh}_2\text{NSiMe}_3)_2]\text{VCl}_2$  (solvent) (1). Method A (Solvent = 2THF).** A solution of  $\text{Li}[\text{CH}(\text{PPh}_2\text{NSiMe}_3)_2]$  was prepared by addition of a solution of MeLi in ether (15.2 mL, 1.4 M, 21.3 mmol) to a solution of  $(\text{Me}_3\text{Si})\text{N}=\text{P}(\text{Ph})_2\text{CHP}(\text{Ph})_2=\text{N}(\text{SiMe}_3)$  (11.9 g, 21.3 mmol) in THF (150 mL) at 0 °C. The resulting solution was added to a suspension of  $\text{VCl}_3(\text{THF})_3$  (7.9 g, 21.3 mmol) in THF (150 mL). A rapid color change took place, resulting in the formation of a dark brown-red solution by the end of the addition. After a further 24 h of stirring at room temperature, the solution was purple, and stirring was continued for an additional 24 h. Since no further color change was observed, the purple solution was concentrated (50 mL) and cooled to -30 °C, upon which purple crystals of **1**·2THF separated (yield: 12.7 g, 15.4 mmol, 72%). Anal. Calcd (found) for  $\text{C}_{39}\text{H}_{54}\text{Cl}_2\text{N}_2\text{O}_2\text{P}_2\text{Si}_2\text{V}$ : C, 56.93 (57.03); H, 6.62 (6.71); N, 3.40 (3.37). IR (Nujol mull,  $\text{cm}^{-1}$ ):  $\nu$  1588 (w), 1440 (s), 1312 (w), 1252 (s), 1170 (s), 1113 (s), 1062 (s),

1027 (w), 999 (w), 954 (s, sh), 844 (s, br), 786 (m), 769 (m), 743 (m), 715 (m), 694 (m), 664 (m), 630 (w), 551 (m).  $\mu_{\text{eff}} = 2.86 \mu_{\text{B}}/\text{mol}$ .

**Method B. Isolation of 1·1.5(toluene) and of  $[\text{VCl}_4(\text{TMEDA})]_2[\text{H}_2(\text{TMEDA})]$  (2).** A solution of  $\text{VCl}_3(\text{THF})_3$  (6.3 g, 16.7 mmol) in THF (70 mL) was treated with  $[\text{CH}_2(\text{PPh}_2\text{NSiMe}_3)_2]$  (4.7 g, 8.4 mmol) and TMEDA (1.9 mL, 12.6 mmol). The solution turned red-purple and was stirred for 24 h. After removal of THF in vacuo, the residual solid was redissolved in warm toluene (150 mL) and the solution filtered. The purple filtrate was allowed to stand at -30 °C for 1 day, upon which blue-purple crystals of **1**·1.5(toluene) separated (1.2 g, 1.5 mmol, 17.5%). Anal. Calcd (found) for  $\text{C}_{41.5}\text{H}_{51}\text{Cl}_2\text{N}_2\text{P}_2\text{Si}_2\text{V}$ : C, 60.95 (60.83); H, 6.29 (6.15); N, 3.43 (3.39).  $\mu_{\text{eff}} = 2.83 \mu_{\text{B}}$ .

The toluene-insoluble residue was redissolved in THF (70 mL), and the solution was filtered, concentrated (20 mL), and allowed to stand at room temperature overnight, upon which red-purple crystals of **2** separated (1.8 g, 2.5 mmol, 58%). Anal. Calcd (found) for  $\text{C}_{18}\text{H}_{50}\text{N}_6\text{Cl}_8\text{V}_2$ : C, 29.37 (29.86); H, 6.85 (7.03); N, 11.42 (11.27). IR (Nujol mull,  $\text{cm}^{-1}$ ):  $\nu$  3674 (w), 1345 (w), 1261 (m), 1098 (m), 1009 (s), 950 (m), 923 (w), 849 (s), 801 (s), 723 (w), 681 (w).  $\mu_{\text{eff}} = 4.23 \mu_{\text{B}}/\text{mol}$ .

**Preparation of  $[\text{CH}(\text{PPh}_2\text{NSiMe}_3)_2]\text{V}(\text{CH}_3)_2$  (3).** A solution of MeLi in ether (9.1 mL, 1.4 M, 12.7 mmol) was added to a purple solution of **1**·2THF (5.2 g, 6.3 mmol) in THF (150 mL) cooled to 0 °C. The color rapidly changed upon mixing from purple to burgundy red, and the solution was slowly warmed to room temperature. After the mixture was stirred for 24 h, THF was removed in vacuo and the residual solid redissolved in ether (80 mL). A small amount of pale-colored solid was removed by centrifugation. Concentration of the ether solution to small volume (20 mL) and further standing at room temperature for 48 h afforded dark red crystals of **3** (yield: 3.3 g, 5.2 mmol, 82%). Anal. Calcd (found) for  $\text{C}_{33}\text{H}_{45}\text{N}_2\text{P}_2\text{Si}_2\text{V}$ : C, 62.05 (61.86); H, 7.10 (7.23); N, 4.39 (4.27). IR (Nujol mull,  $\text{cm}^{-1}$ ):  $\nu$  2853 (vs), 1589 (w), 1437 (s), 1304 (w), 1261 (sh), 1247 (s), 1173 (sh), 1110 (s), 1076 (s), 1056 (s), 1025 (s), 962 (s), 840 (s), 800 (m), 766 (m), 740 (m), 712 (m), 689 (m), 663 (m), 624 (m), 552 (m).  $\mu_{\text{eff}} = 2.76 \mu_{\text{B}}/\text{mol}$ .

**Preparation of  $[\text{CH}(\text{PPh}_2\text{NSiMe}_3)_2]\text{V}_2(\mu\text{-H})_2$  (4).** A burgundy red solution of **3** (0.4 g, 0.6 mmol) in toluene (80 mL) was pressurized in an autoclave with hydrogen (60 atm) for 24 h and at room temperature. The color changed to dark brown-red. The solvent was removed in vacuo and the solid residue redissolved in ether (80 mL). Concentration of the resulting brown-red ether solution (20 mL) and standing for 24 h at room temperature afforded brown crystals of **4** (0.2 g, 0.16 mmol, 52%). Anal. Calcd (found) for  $\text{C}_{62}\text{H}_{80}\text{N}_4\text{P}_4\text{Si}_4\text{V}_2$ : C, 61.07 (61.41); H, 6.61 (6.81); N, 4.59 (4.83). IR (Nujol mull,  $\text{cm}^{-1}$ ):  $\nu$  1950 (w), 1896 (w), 1773 (w), 1589 (w), 1306 (w), 1261 (m), 1154 (s), 1107 (s, br), 1024 (s), 947 (m), 830 (s, br), 741 (m), 717 (m), 691 (m, sh), 653 (m), 605 (m, sh), 548 (w).  $\mu_{\text{eff}} = 1.82 \mu_{\text{B}}/\text{mol}$ .

**Preparation of  $[\text{HC}(\text{PPh}_2\text{N})(\text{PPh}_2\text{NSiMe}_3)\text{V}(\text{OSiMe}_3)]_2\cdot 2\text{Et}_2\text{O}$  (5).** The addition of water (10  $\mu\text{L}$ , 0.6 mmol) to a dark brown solution of **4** (0.4 g, 0.3 mmol) in toluene (50 mL) changed the color to dark red upon mixing. The solvent was removed in vacuo, and the remaining residue was redissolved in ether (60 mL). Dark red crystals of **5** separated (0.14 g, 0.1 mmol, 33%) upon concentration and standing overnight at room temperature. Anal. Calcd (found) for  $\text{C}_{35}\text{H}_{49}\text{N}_2\text{P}_2\text{Si}_2\text{O}_2\text{V}$ : C, 63.04 (63.46); H, 7.41 (7.52); N, 4.20 (4.02). IR (Nujol mull,  $\text{cm}^{-1}$ ):  $\nu$  1588 (w), 1482 (m), 1436 (s), 1377 (s), 1310 (m), 1246 (s), 1173 (s), 1111 (s), 1085 (s), 1046 (m), 1026 (m), 987 (s, br), 790 (w), 771 (m), 742 (m), 723 (m), 694 (m), 667 (m, sh), 617 (m), 555 (m), 533 (w).  $\mu_{\text{eff}} = 2.21 \mu_{\text{B}}/\text{mol}$ .

**Preparation of  $[\text{CH}(\text{PPh}_2\text{NSiMe}_3)_2]\text{V}_2(\mu\text{-Cl})_2(\mu\text{-H})^{-1}/2\text{Et}_2\text{O}$  (6).** A solution of MeLi in ether (1.1 mL, 1.4 M, 1.5 mmol) was added to a purple solution of **1**·2THF (1.3 g, 1.6 mmol) in THF (70 mL) at 0 °C. At the end of the addition the color was red-purple. The solution was warmed slowly to room

(10) Clancy, G. P.; Clark, H. C. S.; Clentsmith, G. K. B.; Cloke, F. G. N.; Hitchcock, P. B. *J. Chem. Soc., Dalton Trans.* **1999**, 19, 3345.

(11) Ong, C. M.; Mckarns, P.; Stephan, D. M. *Organometallics* **1999**, 18, 4197.

(12) Al-Benna, S.; Sarsfield, M. J.; Thornton-Pett, M.; Ormsby, D. L.; Maddox, P. J.; Brès, P.; Bochmann, M. *J. Chem. Soc., Dalton Trans.* **2000**, 23, 3345.

(13) See for example: (a) Kasani, A.; McDonald, R.; Cavell, R. G. *Organometallics* **1999**, 18, 3775. (b) Kasani, A.; McDonald, R.; Ferguson, M.; Cavell, R. G. *Organometallics* **1999**, 18, 4241. (c) Kasani, A.; McDonald, R.; Cavell, R. G. *Chem. Commun.* **1999**, 19, 1993.

(14) Manzer, L. E. *Inorg. Synth.* **1982**, 21, 138.

(15) Appel, V. R.; Ruppert, I. *Z. Anorg. Allg. Chem.* **1974**, 406, 131.

(16) Mabbs, M. B.; Machin, D. *Magnetism and Transition Metal Complexes*; Chapman and Hall: London, 1973.

(17) Foese, G.; Gorter, C. J.; Smits, L. J.; *Constantes Sélectionnées Diamagnétisme, Paramagnétisme, Relaxation Paramagnétique*; Masson: Paris, 1957.

**Table 1. Crystal Data and Structure Analysis Results**

	<b>3</b>	<b>4</b>	<b>5</b>	<b>6</b>	<b>7</b>
formula	C <sub>33</sub> H <sub>45</sub> N <sub>2</sub> P <sub>2</sub> Si <sub>2</sub> V	C <sub>62</sub> H <sub>80</sub> N <sub>4</sub> P <sub>4</sub> Si <sub>4</sub> V <sub>2</sub>	C <sub>70</sub> H <sub>98</sub> N <sub>4</sub> O <sub>4</sub> P <sub>4</sub> Si <sub>4</sub> V <sub>2</sub>	C <sub>64</sub> H <sub>84</sub> Cl <sub>2</sub> N <sub>4</sub> O <sub>0.5</sub> P <sub>4</sub> Si <sub>4</sub> V <sub>2</sub>	C <sub>66</sub> H <sub>90</sub> ClN <sub>4</sub> OP <sub>4</sub> Si <sub>4</sub> V <sub>2</sub>
fw	638.77	1219.42	1397.64	1326.37	1328.99
space group	monoclinic, <i>P2<sub>1</sub>/c</i>	orthorhombic, <i>Pbca</i>	monoclinic, <i>P2<sub>1</sub>/n</i>	monoclinic, <i>P2<sub>1</sub>/n</i>	orthorhombic, <i>Pccn</i>
<i>a</i> (Å)	12.205(2)	15.7893(12)	15.336(2)	16.872(3)	12.120(1)
<i>b</i> (Å)	20.914(3)	17.8846(14)	12.965(1)	20.390(3)	22.416(3)
<i>c</i> (Å)	14.899(2)	22.6540(18)	19.537(2)	22.209(4)	27.168(3)
$\beta$ (deg)	112.785(3)	90	104.225(2)	100.758(3)	90
<i>V</i> (Å <sup>3</sup> )	3506.2(2)	6397.2(9)	3765.6(6)	7506(2)	7381(1)
<i>Z</i>	4	4	2	4	4
radiation (K, Å)	0.710 73	0.710 73	0.710 73	0.710 73	0.710 73
<i>T</i> (K)	203(2)	203(2)	203(2)	203(2)	203(2)
<i>D</i> <sub>calcd</sub> (g cm <sup>-3</sup> )	1.210	1.266	1.233	1.174	1.196
$\rho$ <sub>calcd</sub> (cm <sup>-1</sup> )	4.66	5.08	4.44	5.07	4.81
<i>F</i> <sub>000</sub>	1352	2568	1480	2784	2804
<i>R</i> , <i>R</i> <sub>w</sub> <sup>a</sup>	0.0422, 0.0866	0.0392, 0.0857	0.0479, 0.1022	0.0809, 0.2128	0.0518, 0.1565
GOF	1.015	1.030	1.014	1.016	1.072

$$^a R = \sum F_o - F_c / \sum F_o; R_w = [\sum (F_o - F_c)^2 / \sum w F_o^2]^{1/2}.$$

temperature and allowed to stand at room temperature for 24 h. The solvent was removed in vacuo and the residue redissolved in toluene (80 mL). A small amount of pale-colored insoluble material was removed by centrifugation and the purple-red solution placed in an autoclave and pressurized with H<sub>2</sub> gas (60 atm) for 24 h at room temperature. The solution changed to dark brown-red. The solvent was removed in vacuo, and ether (80 mL) was added to the remaining dark brown residue. After centrifugation, the dark brown-red solution was concentrated to a small volume (20 mL) and allowed to stand for 24 h at room temperature, upon which yellowish brown crystals of **6** formed (yield: 0.65 g, 0.5 mmol, 62%). Anal. Calcd (found) for C<sub>64</sub>H<sub>84</sub>Cl<sub>2</sub>N<sub>4</sub>P<sub>4</sub>Si<sub>4</sub>V<sub>2</sub>O<sub>0.5</sub>: C, 57.95 (58.12); H, 6.38 (6.53); N, 4.22 (4.14). IR (Nujol mull, cm<sup>-1</sup>):  $\nu$  1960 (w), 1944 (w), 1895 (w), 1602 (w), 1589 (w), 1573 (w), 1308 (m), 1243 (s), 1069 (s), 1027 (m, sh), 999 (m, sh), 929 (s), 856 (s), 796 (m, sh), 762 (m, br), 710 (m, br), 656 (m), 627 (m), 600 (m), 548 (m), 507 (m).  $\mu_{\text{eff}} = 1.95 \mu_{\text{B}}/\text{mol}$ .

**Preparation of [CH(PPh<sub>2</sub>NSiMe<sub>3</sub>)<sub>2</sub>V<sub>2</sub>( $\mu$ -Cl)( $\mu$ -H)<sub>2</sub>·Et<sub>2</sub>O (**7**).** A solution of MeLi in ether (1 mL, 1.4 M, 1.4 mmol) was added to a purple solution of **1**·2THF (0.8 g, 0.97 mmol) in THF (70 mL) at 0 °C. At the end of the addition, the color was red-purple. The solution was warmed slowly to room temperature, and stirring was continued for 24 h. The solvent was removed in vacuo, and toluene (80 mL) was added to the residue. A small amount of pale-colored solid was separated by centrifugation, and the purple-red solution was placed in an autoclave and pressurized with H<sub>2</sub> gas (60 atm) for 24 h at room temperature. The solution changed to dark brown-red. The solvent was removed in vacuo and the residue redissolved in ether (80 mL). After centrifugation, the dark brown-red solution was concentrated to a small volume (20 mL) and allowed to stand for 24 h at room temperature, upon which yellowish brown crystals of **7** separated (yield: 0.36 g, 0.3 mmol, 56%). Anal. Calcd (found) for C<sub>66</sub>H<sub>90</sub>ClN<sub>4</sub>P<sub>4</sub>Si<sub>4</sub>V<sub>2</sub>O: C, 59.65 (60.23); H, 6.83 (6.92); N, 4.22 (4.17). IR (Nujol mull, cm<sup>-1</sup>):  $\nu$  1962 (w), 1890 (w), 1582 (w), 1256 (sh), 1245 (sh), 1146 (s, br), 1100 (s, br), 1027 (w, sh), 924 (w, sh), 839 (s), 796 (w), 760 (m), 741 (m), 722 (m), 709 (m), 658 (w), 597 (w).  $\mu_{\text{eff}} = 1.88 \mu_{\text{B}}/\text{mol}$ .

**X-ray Crystallography. Structural Determination of 3–7.** Suitable crystals were selected, mounted on thin, glass fibers using paraffin oil, and cooled to the data collection temperature. Data were collected on a Bruker AX SMART 1K CCD diffractometer using 0.3°  $\omega$ -scans at 0, 90, and 180° in  $\phi$ . Unit-cell parameters were determined from 60 data frames collected at different sections of the Ewald sphere. Semiempirical absorption corrections based on equivalent reflections were applied.<sup>18</sup> Systematic absences in the diffraction data and unit-cell parameters were uniquely consistent with the re-

ported space groups. The structures were solved by direct methods, completed with difference Fourier syntheses, and refined with full-matrix least-squares procedures based on  $F^2$ . The compound molecule in **7** was located at a 2-fold axis, while each compound molecule in **5** and **4** was located at an inversion center. One cocrystallized diethyl ether solvent molecule was found in each asymmetric unit of **5**, half-occupied in **6**, and disordered over a 2-fold axis in **7**. Hydride ligands for **7** and **6** were initially located from the difference map and refined with a riding model. All other hydrogen atoms were treated as idealized contributions. A hydride ligand and a chloride ligand were each found to be disordered by a 2-fold axis in **7**. All non-hydrogen atoms were refined with anisotropic displacement parameters. All scattering factors and anomalous dispersion factors are contained in the SHELXTL 5.10 program library.<sup>19</sup> Crystal data and relevant bond distances and angles are given in Tables 1 and 2.

**Complex 3.** The complex shows the ligand connected to the metal center via the two nitrogen atoms (V–N(1) = 2.054(3) Å, V–N(2) = 2.048(3) Å) (Figure 1). The carbon atom located between the two phosphorus forms a long V–C distance (V–C(18) = 2.524(3) Å), which may be considered as at the edge of the bonding range. The ligand adopted with the metal center a butterfly type of conformation folded along the V–C vector. The coordination geometry around the vanadium center is distorted trigonal bipyramidal, with the two nitrogen donor atoms and one carbon of one of the two terminally bonded methyl groups (V–C(2) = 2.070(4) Å) defining the trigonal equatorial plane (N(1)–V–N(2) = 116.07(11)°, N(1)–V–C(2) = 116.46(13)°, N(2)–V–C(2) = 117.60(13)°). The ligand carbon donor atom and the second methyl group (V–C(1) = 2.120(3) Å) occupy the axial positions (C(1)–V–C(18) = 162.90(13)°).

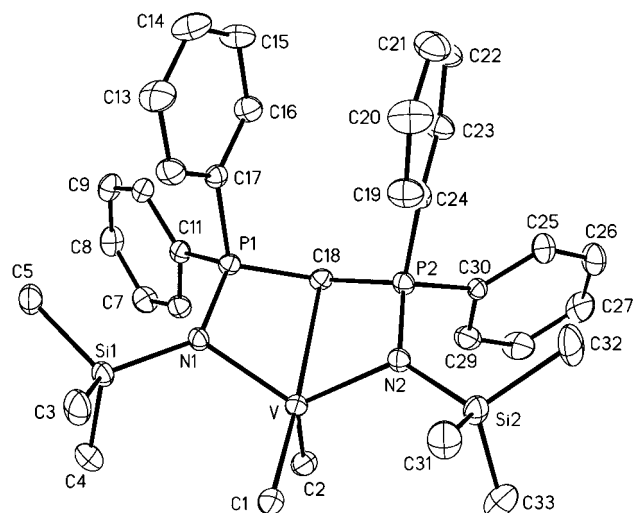
**Complex 4.** The dimeric structure consists of two identical [(Me<sub>3</sub>Si)N=P(Ph)<sub>2</sub>C(H)P(Ph)<sub>2</sub>=N(SiMe<sub>3</sub>)]V units where the ligand adopted the usual geometry folded along the V–C<sub>ligand</sub> vector (V(1)–C(16) = 2.381(2) Å) (Figure 2). The structure was of sufficient quality to allow location with a reasonable degree of confidence the positions of the hydrogen atoms, including those of the two bridging hydrides. The two hydrides bridge the two vanadium atoms (V(1)–H(1) = 1.74(2) Å, V(1)–H(1a) = 2.180(2) Å), forming a planar V<sub>2</sub>H<sub>2</sub> core (torsion angle V(1)–H(1)–V(1a)–H(1a) = 0°) with a rather short V–V distance (V(1)–V(1a) = 2.4569(7) Å). The coordination geometry around each vanadium center is severely distorted trigonal bipyramidal. The equatorial plane is defined by the two nitrogen donor atoms (V(1)–N(1) = 2.141(2) Å; V(1)–N(2) = 2.186(2) Å) and one hydride, forming a distorted trigonal plane with the vanadium atom (N(1)–V(1)–N(2) = 107.13(7)°, N(1)–V(1)–H(1a) = 133.87(7)°, N(2)–V(1)–H(1a) = 108.32(7)°). The two axial positions are occupied by the ligand carbon atom and

(18) Blessing, R. *Acta Crystallogr.* **1995**, *A51*, 33.

(19) Sheldrick, G. M. Bruker AXS, Madison, WI, 1997.

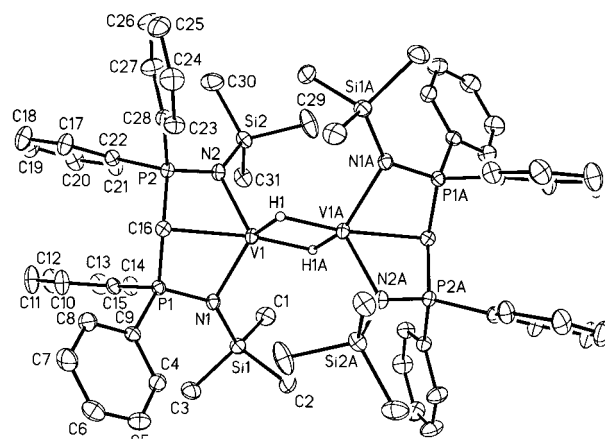
**Table 2. Selected Bond Distances (Å) and Angles (deg)**

Compound 3							
V–N(2)	2.045(3)	V–C(1)	2.120(3)	V–P(1)	2.8118(11)	P(1)–N(1)	1.618(3)
V–N(1)	2.048(3)	V–C(18)	2.524(3)	V–P(2)	2.8201(11)	P(1)–C(18)	1.726(3)
V–C(2)	2.070(4)						
N(2)–V–N(1)	116.07(11)	N(2)–V–C(1)	100.93(13)	N(2)–V–C(18)	71.58(11)	C(2)–V–C(18)	95.50(13)
N(2)–V–C(2)	117.60(13)	N(1)–V–C(1)	100.21(12)	N(1)–V–C(18)	71.82(11)	C(1)–V–C(18)	163.90(13)
N(1)–V–C(2)	116.46(13)	C(2)–V–C(1)	100.60(15)				
Compound 4							
V(1)–H(1)	1.741(2)	V(1)–N(2)	2.1859(18)	V(1)–P(11)	2.7743(7)	P(1)–C(16)	1.743(2)
V(1)A–H(1)	1.802(2)	V(1)–C(16)	2.381(2)	V(1)–P(2)	2.8174(7)	P(1)–C(9)	1.822(2)
V(1)–N(1)	2.1410(19)	V(1)–V(1)A	2.4569(7)	P(1)–N(1)	1.5926(18)		
V(1)–H(1)–V(1)A	87.80(7)	N(1)–V(1)–V(1)A	126.74(5)	N(1)–V(1)–P(1)	34.89(5)	V(1)A–V(1)–P(1)	149.90(3)
N(1)–V(1)–N(2)	107.13(7)	N(2)–V(1)–V(1)A	119.54(5)	N(2)–V(1)–P(1)	90.26(5)	N(1)–V(1)–P(2)	96.78(5)
N(1)–V(1)–C(16)	73.46(7)	C(16)–V(1)–V(1)A	143.34(5)	C(16)–V(1)–P(1)	38.57(5)	N(2)–V(1)–P(2)	34.27(5)
N(2)–V(1)–C(16)	71.26(7)						
Compound 5							
V(1)–O(1)	1.860(3)	V(1)–N(1)	2.036(4)	V(1)–V(1)A	2.7828(16)	P(1)–C(16)	1.727(5)
V(1)–N(2)	1.946(4)	V(1)–C(16)	2.485(5)	V(1)–P(2)	2.7968(16)	P(1)–C(22)	1.800(5)
V(1)–N(2)A	2.011(4)	V(1)–P(1)	2.7142(16)	P(1)–N(2)	1.593(4)	V(1)A–N(2)	2.011(4)
O(1)–V(1)–N(2)	121.36(15)	N(2)A–V(1)–N(1)	103.75(15)	O(1)–V(1)–P(1)	111.94(11)	O(1)–V(1)–V(1)A	121.37(11)
O(1)–V(1)–N(2)A	102.52(15)	O(1)–V(1)–C(16)	97.41(15)	N(2)–V(1)–P(1)	35.35(11)	N(2)–V(1)–V(1)A	46.28(11)
N(2)–V(1)–N(2)A	90.64(15)	N(2)–V(1)–C(16)	73.66(16)	N(2)A–V(1)–P(1)	125.47(12)	N(2)A–V(1)–V(1)A	44.37(11)
O(1)–V(1)–N(1)	116.89(15)	N(2)A–V(1)–C(16)	159.17(16)	N(1)–V(1)–P(1)	96.87(11)	N(1)–V(1)–V(1)A	117.55(12)
N(2)–V(1)–N(1)	114.57(16)	N(1)–V(1)–C(16)	71.90(16)	C(16)–V(1)–P(1)	38.48(11)		
Compound 6							
V(1)–H(1)	1.902(10)	V(1)–Cl(2)	2.434(4)	V(1)–P(1)	2.840(3)	V(2)–Cl(1)	2.386(3)
V(1)–N(2)	2.193(8)	V(1)–Cl(1)	2.474(3)	V(2)–N(3)	2.055(9)	V(2)–Cl(2)	2.414(4)
V(1)–N(1)	2.277(8)	V(1)–V(2)	2.754(3)	V(2)–N(4)	2.147(8)	V(2)–P(3)	2.756(3)
V(1)–C(13)	2.353(11)	V(1)–P(2)	2.800(3)	V(2)–C(44)	2.332(10)	V(2)–P(4)	2.789(3)
V(1)–H(1)–V(2)	92.8(3)	N(2)–V(1)–Cl(2)	96.6(2)	N(1)–V(1)–Cl(1)	91.9(2)	N(1)–V(1)–V(2)	139.0(2)
N(2)–V(1)–N(1)	93.8(3)	N(1)–V(1)–Cl(2)	107.6(2)	C(13)–V(1)–Cl(1)	104.4(3)	C(13)–V(1)–V(2)	133.7(3)
N(2)–V(1)–C(13)	72.4(3)	C(13)–V(1)–Cl(2)	168.6(3)	Cl(2)–V(1)–Cl(1)	86.85(11)	Cl(2)–V(1)–V(2)	55.04(9)
N(1)–V(1)–C(13)	70.6(3)	N(2)–V(1)–Cl(1)	172.2(3)	N(2)–V(1)–V(2)	122.8(2)		
Compound 7							
V(1)–H(1)	1.647(2)	V(1)–N(1)	2.227(2)	V(1)–V(1)A	2.6518(8)	Cl–V(1)A	2.3878(11)
V(1)–H(2)	1.684(2)	V(1)–C(16)	2.338(2)	V(1)–P(2)	2.8012(8)	P(1)–N(1)	1.588(2)
V(1)A–H(2)	1.676(2)	V(1)A–Cl	2.3878(11)	V(1)–P(1)	2.8045(8)	P(1)–C(16)	1.744(3)
V(1)–N(2)	2.155(2)	V(1)–Cl	2.4532(12)				
V(1)–H(1)–V(1)A	107.26(10)	N(2)–V(1)A–Cl	96.62(6)	N(1)–V(1)–Cl	90.21(6)	N(1)–V(1)–V(1)A	138.02(6)
V(1)–H(2)–V(1)A	104.22(10)	N(1)–V(1)A–Cl	103.18(7)	C(16)–V(1)–Cl	102.40(6)	C(16)–V(1)–V(1)A	134.53(6)
N(2)–V(1)–N(1)	93.67(8)	C(16)–V(1)A–Cl	166.63(6)	Cl–V(1)A–Cl	89.16(5)	ClA–V(1)–V(1)A	57.98(3)
N(2)–V(1)–C(16)	72.57(8)	N(2)–V(1)–Cl	172.12(7)	N(2)–V(1)–V(1)A	123.55(6)	Cl–V(1)–V(1)A	55.61(3)
N(1)–V(1)–C(16)	70.48(8)						

**Figure 1.** Partial thermal ellipsoid plot of **3**. Thermal ellipsoids are drawn at the 30% probability level.

by the second bridging hydride, featuring a bent H–V–C array (C(16)–V(1)–H(1a) = 170.95(7)°). The V–H distances are slightly different, as a possible result of the asymmetric arrangement of the two hydrides, each occupying an equatorial position with respect to one vanadium and an axial position with respect to the second one.

**Complex 5.** The complex is a dimer formed by two vanadium moieties attached to the ligand, where one of the two nitrogen atoms no longer bears the silyl group (Figure 3). This

**Figure 2.** Thermal ellipsoid plot of **4**. Thermal ellipsoids are drawn at the 30% probability level.

particular nitrogen atom bridges the vanadium atom of an identical unit, assembling a dimeric structure (N(2)–V(1)–N(2a) = 90.64(15)°, V(1)–N(2)–V(1a) = 89.36(20)°) with a planar V<sub>2</sub>N<sub>2</sub> core (torsion angle V(1)–N(2)–V(1)A–N(2a) = 0°). Conversely, the silane group is found attached to an oxygen atom of a terminally bonded trimethylsilylanolate group (V(1)–O(1) = 1.860(3) Å). The coordination geometry around each vanadium atom is trigonal bipyramidal, as a common feature among these derivatives. The equatorial plane is defined by one terminally bonded N atom (V(1)–N(1) = 2.036(4) Å) of the Me<sub>3</sub>SiN group, one bridging desilylated N atom (V(1)–N(2) = 1.946(4) Å), and the oxygen atom of the silanolate group (O(1)–

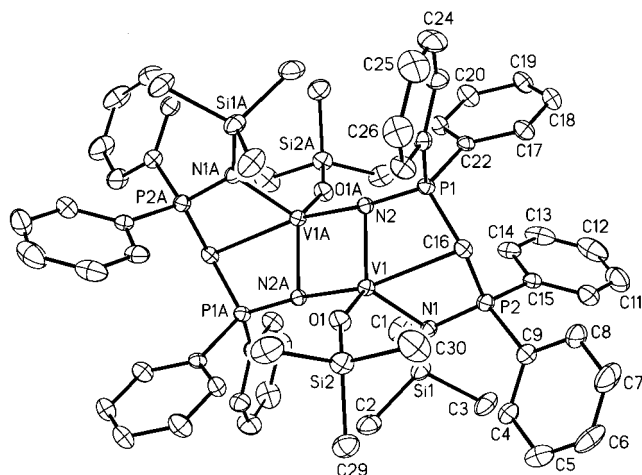


**Figure 3.** Thermal ellipsoid plot of **5**. Thermal ellipsoids are drawn at the 30% probability level.

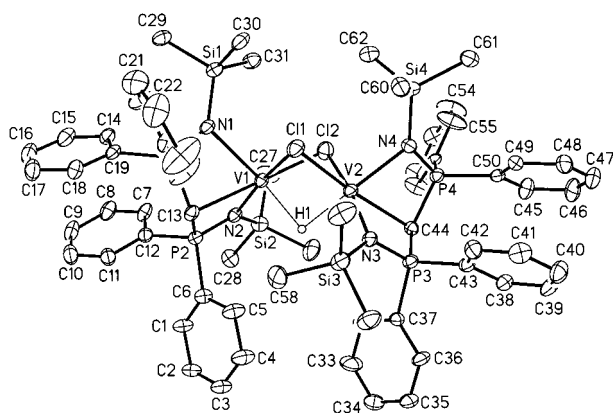


**Figure 4.** Thermal ellipsoid plot of **6**. Thermal ellipsoids are drawn at the 30% probability level.

$V(1)-N(1) = 116.89(15)^\circ$ ,  $O(1)-V(1)-N(2) = 121.36(15)^\circ$ ,  $N(1)-V(1)-N(2) = 114.57(16)^\circ$ . The ligand carbon atom ( $V(1)-C(16) = 2.485(5) \text{ \AA}$ ) and the desilylated N atom of a second unit occupy the axial positions, forming a bent  $N-V-C$  vector ( $N(2)A-V(1)-C(16) = 159.17(16)^\circ$ ). The desilylated N atoms display with the two vanadium atoms and the phosphorus a curious planar T-shaped type of geometry ( $P(1)-N(2)-V(1a) = 167.14(16)^\circ$ ,  $P(1)-N(2)-V(1) = 99.67(16)^\circ$ ,  $V(1)-N(2)-V(1a) = 89.36(20)^\circ$ ).

**Complexes 6 and 7.** The crystal structures of **6** and **7** show the same dinuclear arrangement, with the ligand around each vanadium atom adopting the usual tridentate bonding mode with a folded-butterfly type of conformation (**6**,  $V(1)-N(1) = 2.277(8) \text{ \AA}$ ,  $V(1)-N(2) = 2.193(8) \text{ \AA}$ ; **7**,  $V(1)-N(1) = 2.227(2) \text{ \AA}$ ,  $V(1)-N(2) = 2.155(2) \text{ \AA}$ ) (Figures 4 and 5). Different from **4**, the overall coordination geometry around each vanadium atom in both compounds is octahedral, with three coordination sites occupied by the two nitrogen and carbon atoms (**6**,  $V(1)-C(13) = 2.353(11) \text{ \AA}$ ; **7**,  $V(1)-C(16) = 2.338(2) \text{ \AA}$ ) and the other three occupied by the bridging chlorine (**6**,  $V(1)-Cl(1) = 2.474(3) \text{ \AA}$ ; **7**,  $V(1)-Cl(1) = 2.434(2) \text{ \AA}$ ) and hydride atoms (**6**,  $V(1)-H(1) = 1.902(10) \text{ \AA}$ ; **7**,  $V(1)-H(1) = 1.647(2) \text{ \AA}$ ). In the case of **6**, the two metals are bridged by one hydride ( $V(1)-H(1)-V(2) = 92.8(2)^\circ$ ) and two chlorine atoms ( $V(1)-Cl(1)-V(2) = 69.00(20)^\circ$ ,  $V(1)-Cl(2)-V(2) = 69.21(19)^\circ$ ), while two bridging hydrides ( $V(1)-H(1)-V(1a) = 107.26(20)^\circ$ ,  $V(1)-H(2)-V(1a) = 104.22(18)^\circ$ ) and one chlorine atom ( $V(1)-Cl(1)-V(1a) = 66.41(20)^\circ$ ) are present in the case of **7**. The divanadium units thus adopt in both compounds a face-sharing bioctahedral structure. In complex **7** the chlorine atom appears to be trans

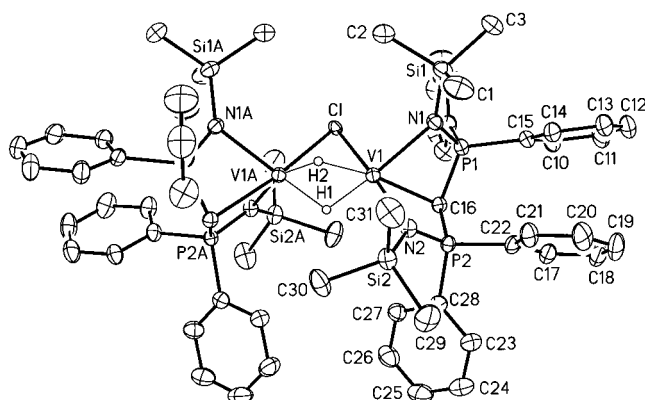
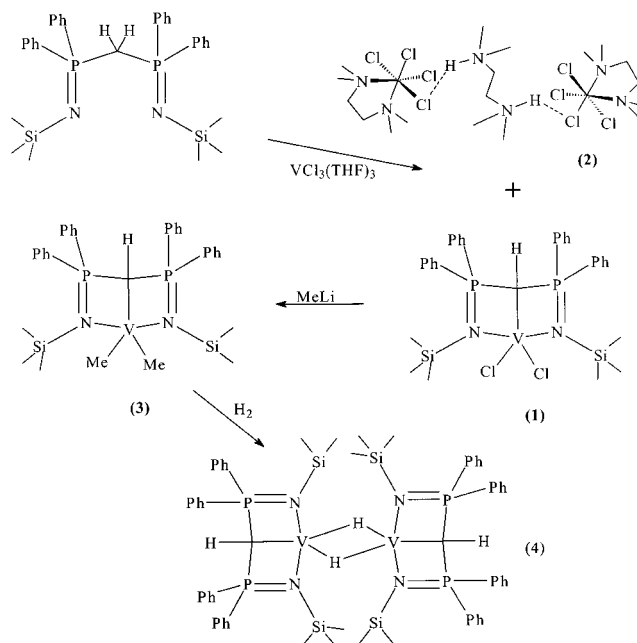


**Figure 5.** Thermal ellipsoid plot of **7**. Thermal ellipsoids are drawn at the 30% probability level.

### Scheme 1

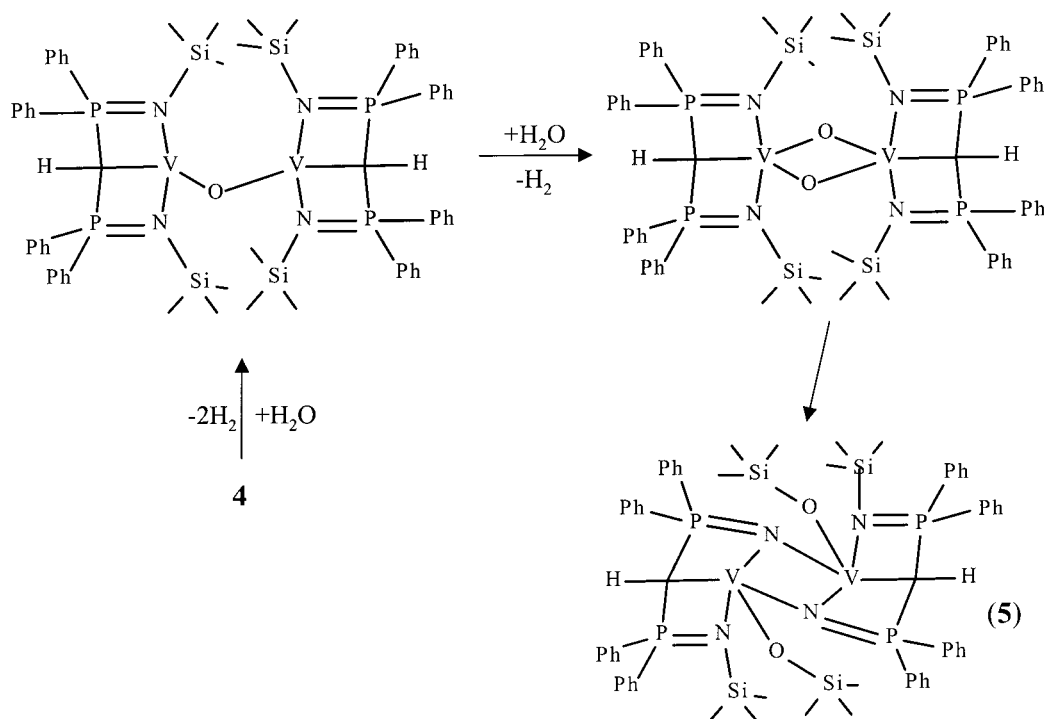


with respect to one N donor atom of one vanadium atom and trans to the  $C_{\text{ligand}}$  atom of the second vanadium-containing moiety.

### Results and Discussion

Reaction of  $VCl_3(THF)_3$  with the diphosphine diimine ligand  $[(Me_3Si)N=P(Ph)_2C(H)_2P(Ph)_2=N(SiMe_3)]$  in its neutral form and in the presence of TMEDA afforded the violet  $[(Me_3Si)N=P(Ph)_2C(H)P(Ph)_2=N(SiMe_3)]VCl_2 \cdot (toluene)$  (**1**·toluene) and the red-purple  $[(TMEDA)-VCl_4]_2[H_2(TMEDA)]$  (**2**) (Scheme 1). Both compounds were isolated in pure form from the same reaction mixture via fractional crystallization from THF and toluene. Analytical data consistent with the proposed formulation were obtained for both compounds and their structures elucidated by X-ray crystallography (see the Supporting Information). The two complexes are paramagnetic and display magnetic moments consistent with a  $d^2$  electronic configuration. Complex **1** was prepared in substantially higher yield (72%) as a THF solvate (**1**·2THF) via direct reaction of the  $VCl_3(THF)_3$  starting material with the monolithium phosphinoimino anion<sup>12</sup> prepared in situ via treatment of  $[(Me_3-$

Scheme 2



Si)N=P(Ph)<sub>2</sub>C(H)<sub>2</sub>P(Ph)<sub>2</sub>=N(SiMe<sub>3</sub>) with 1 equiv of MeLi in ether. The bond distances and angles of the two solvate forms of **1** are identical within the esd values (see the Supporting Information).

Metal complexes of the deprotonated phosphinoimine derivatives are organometallic species only from the *formal* point of view, given that resonance structures with the negative charge localized on the nitrogen rather than on the carbon atom are likely to be the most important. Nonetheless, the coexistence in the reaction mixture of a V(III) species, presumably containing reactive V–N and V–C bonds, with a fairly strong acid such as the ammonium salt of TMEDA is rather surprising and reiterates the unique stability of the derivatives of the pincer-type ligand system.<sup>13</sup> On the other hand, the ammonium acidic protons are tightly coordinated in complex **2** between TMEDA and two VCl<sub>3</sub>(TMEDA) units bridging the TMEDA nitrogen atom and one of the four chlorine atoms bound to the vanadium center. The strong hydrogen bonding may well be responsible for quenching the acidity of the ammonium cation.

Complex **1** was converted into the corresponding isostructural dimethyl derivative [(Me<sub>3</sub>Si)N=P(Ph)<sub>2</sub>C(H)P(Ph)<sub>2</sub>=N(SiMe<sub>3</sub>)]VMe<sub>2</sub> (**3**) via simple treatment with MeLi (Scheme 1) followed by crystallization from ether. This species is also paramagnetic and displays a magnetic moment consistent with a d<sup>2</sup> electronic configuration of a monomeric V(III) derivative. The chelating ligand in complex **3** displays the same geometry as in **1** with comparable bond distances and angles (Figure 1). The most noticeable difference between the two compounds arises from the V–C<sub>ligand</sub> distance (V–C(16) = 2.334(2) Å (**1**) versus V–C(18) = 2.524(3) Å (**3**)). This can in principle be ascribed to steric compression of the ligand, as indicated by the substantial distortions of the bond angles around the carbon bridging the two phosphorus atoms (P(1)–C(18)–P(2) = 127.4(3)°, V–C(18)–

P(1) = 80.46(13)°, V–C(18)–P(2) = 80.74(12)°). However, given that very similar distortions are observed in **1**, which contains a much shorter V–C<sub>ligand</sub> distance, the longer V–C<sub>ligand</sub> distance of **3** is likely to be instead the result of trans influence or of an enhanced contribution of the amido-type resonance structure.

The hydrogenolysis of **3** was performed at room temperature and under pressure (60 atm). The reaction afforded the extremely air-sensitive, divalent, and dinuclear hydride complex {[(Me<sub>3</sub>Si)N=P(Ph)<sub>2</sub>C(H)P(Ph)<sub>2</sub>=N(SiMe<sub>3</sub>)]V<sub>2</sub>(μ-H)<sub>2</sub>} (**4**) (Figure 2), which was isolated as brown crystals in 57% yield. The identity of the product was established by a combination of X-ray crystal structure, elemental analysis, and chemical degradation carried out with anhydrous HCl in a sealed vessel connected to a Toepler pump, which afforded 96% of the expected amount of H<sub>2</sub> gas. The magnetic moment (1.82 μ<sub>B</sub>/mol) is considerably low for a dinuclear d<sup>3</sup> system and is presumably indicative of some direct V–V interaction.

The divalent hydride **4** is a highly reactive species, whose handling has proven to be unusually difficult. We also observed that exposure of either solid samples or solutions of **4** to air turned the samples intensely red. As shown in Scheme 2, reaction of **4** with 2 equiv of water released 87% of the expected 3 equiv of hydrogen gas, affording the new dinuclear and trivalent species {[(Me<sub>3</sub>Si)N=P(Ph)<sub>2</sub>C(H)P(Ph)<sub>2</sub>=N(SiMe<sub>3</sub>)]V<sub>2</sub>(OSiMe<sub>3</sub>)<sub>2</sub>} (**5**), isolated as dark red crystals. Its X-ray crystal structure revealed a dinuclear complex where the ligand was deprived of one of the two SiMe<sub>3</sub> groups attached to the N atom, forming a terminally bonded silanolate group (Figure 3). The complex displayed a rather low paramagnetism (μ<sub>eff</sub> = 2.21 μ<sub>B</sub>/mol), which is consistent with the fairly short V–V distance (V(1)–V(1)A = 2.783(2) Å).

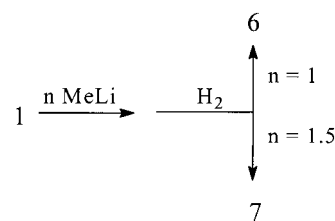
The connectivity of **5**, as yielded by the crystal structure clearly attributes the oxidation state +3 to

each vanadium atom. Thus, the formation of **5** from the divalent **4** involves not only an acid–base reaction but also a one-electron oxidation of each of the two vanadium centers, releasing a total of 3 equiv of hydrogen gas. The reaction can be conveniently rationalized by assuming an initial acid–base reaction of **4** with one molecule of water to afford an intermediate divalent oxo derivative (Scheme 2). This step releases the first 2 equiv of hydrogen. Further reaction with a second molecule of water forms a trivalent dioxo species upon releasing the third equivalent of hydrogen gas. Migration of the oxophilic Me<sub>3</sub>Si group from nitrogen to the oxygen atom affords **5**. The displacement of the Me<sub>3</sub>Si group is rather surprising in this case, in the view of the fact that  $\{[(\text{Me}_3\text{Si})_2\text{N}]_2\text{V}(\mu\text{-O})\}_2$  is a perfectly stable species.<sup>20</sup>

The formation of the divalent **4** from the trivalent **3** again poses questions about the stability of vanadium hydrides. As briefly mentioned in the Introduction, an intrinsic instability of intermediate vanadium alkyls toward presumably unstable trivalent vanadium hydrides is believed to be responsible for polymer chain termination and reduction of the vanadium catalytic site to the inactive divalent state.<sup>8</sup> This process is commonly regarded as catalyst deactivation. To mitigate its negative impact, the current technology for elastomer manufacture employs halogenated organic substances. It is also common belief that the role of this species is that of reoxidizing the inactive divalent metal centers toward the active trivalent state. This oxidation process implies that a chloride anion is transferred to the vanadium center. It is also well established from the patent literature that the presence of chloride ions as a component of the catalytic system is critical to the performance of the catalytic cycle.<sup>8</sup> These observations prompted us to evaluate the stability of mixed hydride/chloride vanadium species. For this purpose, we attempted the preparation of a partially alkylated trivalent  $[(\text{Me}_3\text{Si})\text{N}=\text{P}(\text{Ph})_2\text{C}(\text{H})\text{P}(\text{Ph})_2=\text{N}(\text{SiMe}_3)]\text{V}(\text{Cl})\text{Me}$  species for further hydrogenolysis. Unfortunately, the isolation of methyl/chloride precursors only afforded a mixture of **1** and **3**. Therefore, it was decided simply to mix the starting dichloride **1** with the appropriate amount of MeLi and to carry out the hydrogenolysis of the resulting mixture under the usual reaction conditions (60 atm, room temperature). This strategy proved to be successful for the isolation in crystalline form of two new mixed-valent vanadium hydride/chloride species depending on the stoichiometric V/MeLi ratio employed for the reaction.

Reaction of **1** with either 1.0 or 1.5 equiv of MeLi followed by hydrogenolysis of the resulting solutions afforded the dinuclear and mixed-valence V(II)/V(III) species  $\{[(\text{Me}_3\text{Si})\text{N}=\text{P}(\text{Ph})_2\text{C}(\text{H})\text{P}(\text{Ph})_2=\text{N}(\text{SiMe}_3)]\text{V}\}_2(\mu\text{-Cl})_2(\mu\text{-H})$  (**6**) (Figure 4) and  $\{[(\text{Me}_3\text{Si})\text{N}=\text{P}(\text{Ph})_2\text{C}(\text{H})\text{P}(\text{Ph})_2=\text{N}(\text{SiMe}_3)]\text{V}\}_2(\mu\text{-Cl})(\mu\text{-H})_2$  (**7**) (Figure 5), respectively (Scheme 3). Both compounds were isolated in analytically pure form as extremely air-sensitive brown crystalline solids and released the expected amount of hydrogen gas upon decomposition with gaseous HCl. The most noticeable difference between the two compounds consists of the V–V distances (**6**, V(1)–V(2) =

Scheme 3



2.754(3) Å; **7**, V(1)–V(1a) = 2.6518(8) Å), which obviously are exclusively determined by the number of bridging chlorine atoms. The substantial variation of intermetallic distances does not correspond to a significant variation of the magnetic moments, which are comparable in the two compounds and are in both cases consistent with the presence of one unpaired electron per dimeric unit.

The divalent state of vanadium in **4** is in striking contrast with the mixed-valence nature of **6** and **7** and clearly demonstrates the ability of the chlorine atom to prevent complete reduction toward the divalent state. Although the formation of the monohydride dichloride **6** could be regarded as the result of the direct reaction of **1** with in situ generated **4**, this obviously cannot be the case for **7**, which contains *two* hydrides and *one* chloride. Furthermore, there is no apparent reason complex **4** could not exist as a mixed-valence V(II)/V(III) species with three bridging hydrides and a face-sharing biocathedral structure similar to that of **6** and **7**. Indeed, the retention of chlorine is a factor preventing reduction toward the divalent state.

## Conclusions

The monoanionic “pincer”-type ligand  $[(\text{Me}_3\text{Si})\text{N}=\text{P}(\text{Ph})_2\text{C}(\text{H})\text{P}(\text{Ph})_2=\text{N}(\text{SiMe}_3)]$  afforded stabilization of rare examples of trivalent vanadium dialkyls and mixed-valence and divalent hydrides. The three hydride derivatives **4**, **6**, and **7** have been obtained through identical reactions, the only difference being the amount of residual chlorine present in the reaction mixture. Thus, the role of chlorine in terms of stabilizing higher oxidation states and preventing reduction toward divalent state becomes apparent. It is tempting at this stage to speculate that the crucial role of chlorine in promoting and optimizing the performance of vanadium as a Ziegler–Natta catalyst relies on its ability to assemble polymetallic structures where, similar to the case of **6** and **7**, the preservation of the trivalent oxidation state results in an extended catalyst life.

**Acknowledgment.** This work was supported by the Natural Science and Engineering Council of Canada (NSERC).

**Supporting Information Available:** Complete listings of structural parameters and crystal data for the complexes. This material is available free of charge via the Internet at <http://pubs.acs.org>.

(20) Duan, Z.; Schmidt, M.; Young, V. G.; Xie, X.; McCarley, R. E.; Verkade, J. G. *J. Am. Chem. Soc.* **1996**, *118*, 5302.